SIGNATURES OF SENTINEL-1 RADAR AND SMAP RADIOMETER DEPENDING ON THE TEMPERATURE OF FROZEN ARCTIC SOIL IN THE COOLING AND HEATING PROCESS OF THE ACTIVE LAYER

K.V. Muzalevskiy, Z. Ruzicka

Kirensky Institute of Physics Federal Research Center KSC SB RAS,
660036 Krasnoyarsk, the Russian Federation

ABSTRACT

In this paper, the results of radiothermal and radar remote sensing of several Arctic tundra test sites were investigated to establish the dependences of the reflectivity and backscattering coefficient on soil temperature. The brightness temperature and backscattering coefficient were measured by a SMAP radiometer (1.4GHz) and Sentinel-1 radar (5.4GHz) over areas near to Franklin Bluffs weather station in the North Slope of Alaska and Isachsen weather station on Ellef Ringnes Island respectively. It has been experimentally and theoretically shown that between the surface soil temperature measured by weather stations in the period 2015-2016 and the reflectivity or backscattering coefficient there is a strong correlation relationship no worse than 0.68. In addition, in the range of soil surface temperature changes from -30°C to 0°C, the variations in the backscattering coefficient and reflectivity are about 4 dB for both test sites. This study contributes to further understanding the processes of microwave emission and scattering of frozen Arctic soils that is pertinent to developing new remote sensing algorithms for the permafrost region.

Index Terms— SMAP, Sentinel-1, microwave radiometry, radar backscattering, Arctic tundra, active layer, soil moisture, soil temperature, permittivity model.

1. INTRODUCTION

The surface soil temperature, soil moisture, permafrost thermal state and timing of the seasonally frozen and thawed states of the soil surface are included in the fifty-four essential climate variables recommended by the World Meteorological Organization for observation [1]. These parameters-indicators which are may capable characterizing the integrated impact of anthropogenic and natural factors on the Arctic ecosystem. At the same time, especially in the Arctic region, weather station networks are too sparse to provide enough data to climatic models about soil temperature, soil moisture and permafrost state. Modern remote sensing satellites passing close to polar orbits can observe up to several times a day extensive arctic areas with high spatial resolution. They are an additional source of independent data, complementing the highly sparse ground-based measurements of meteorological stations. At the same time, insufficient knowledge of the processes of microwave emission and scattering microwaves by the Arctic tundra soils hindered remote sensing of these parameters because of a significant error in their measurement in polar regions [2]-[5]. In this paper, the dependences of radiothermal emission in the L-band and radar backscattering in the C-band on the soil temperature during cooling and heating of the frozen active layer were investigated at several test sites in the Arctic tundra. These temperature dependences are related to the phase transitions of water in the process of cooling and heating of frozen soil [6]. Temperature dependences of complex permittivity (CDP) are well studied during the thawing and freezing of soil samples with a high content of organic matter in laboratory conditions [6]. Such temperature-dependent changes in CDP can to provide measuring not only the thawed or frozen soil states, but also to determine content of unfrozen water and ice, as well as temperature of frozen soil during it cooling and heating process. Before, the temperature dependence of the backscattering coefficient, measured by Sentinel-1 and Radarsat, for mineral soils of moderate latitudes was studied in [7], [8]; for the Arctic region, these studies were not performed.

2. TEST SITE AND SATELLITES DATA

The areas next to Franklin Bluffs weather station (FBS) in the North Slope of Alaska (NSA) and Isachsen weather station (IS) on the western shore of Ellef Ringnes Island were selected as Arctic tundra test sites. The coordinates of FBS and IS are (69.6741,-148.7208) and (78.7833,-103.5500) respectively. FBS and IS sites are located on the inner coastal plain with river terraces. Landcover units in the FBS area include Graminoid-moss tundra and graminoid, prostrate-dwarf-shrub, and moss tundra (wet and moist nonacidic). Included in the IS area are the prostrate dwarf shrub and Salix arctica, which is rare and the height of the vegetation is no more than approximately 10 cm [9]. Time

series temperature and moisture data for the active layer, air temperature and snow depth has been recorded for these sites over a relatively long period (2008-2017) [10]. For radar observations, the area of the IS meteorological station was chosen, which is uniquely located in the Arctic region. Over the chosen area about a hundred Sentinel-1 images are available, unlike other test sites that there are weather stations, but few radar data are available (e.g. in the North Slope of Alaska). However, due to the small size and mountainous terrain in the IS test site, it is not possible to use the brightness temperature data of the SMAP radiometer (40x40 km in spatial resolution). In connection with this, for brightness temperature observations the FBS weather station in NSA was selected, which is sufficiently far from the coastline and from the Brooks Range. In this paper, SMAP and Sentinel-1 observations covered the period from April 1, 2015 to May 29, 2016 and from May 22, 2015 to December 19, 2017 respectively were used. For these periods were analysed 320 and 81 brightness temperature (1.4GHz, incidence angle of ~40°) and radar (5.405GHz, incidence angle of ~30-45+°) images respectively. The brightness temperature for the FBS test site was acquired from an enhanced Level-1C SMAP product (SPL1CTB_E) descending half-orbit passes (aft looks antenna scan). Radar backscattering for the IS test site was acquired from GRD Level-1 Sentinel-1 products with EW (medium resolution) sensor mode, and passes about 14:00 (UTC) and HH-pol were used. Radar images were processed in the Sentinel Application Platform (SNAP) according to the standard procedure: applying precise orbits, thermal noise removal, radiometric calibration, speckle filtering (3x3 mean filter), range Doppler terrain correction (ACE2_5min digital elevation model with UTM Zone 13 projection) and incidence angle normalization (reference angle 40°).

3. SIGNATURES OF RADIOMETER AND RADAR DEPENDING ON THE TEMPERATURE OF FROZEN ARCTIC SOIL IN THE COOLING AND HEATING PROCESS OF THE ACTIVE LAYER

Analysis of the variations in the brightness temperature of the tundra soil were performed using the following model for a dielectrically homogeneous isothermal medium [11]:

$$T_{B,p}(\theta) = \left[1 - \Gamma_p(\vartheta)\right] \cdot T_s, \qquad \Gamma_p(\vartheta) = \left|R_p(\vartheta, \varepsilon_s)\right|^2 e^{-h_r}. \tag{1}$$

Here $p=H$ and $p=V$ signify horizontal and vertical polarizations, T_s is the effective soil temperature, $R_p(\vartheta, \varepsilon_s)$ is the Fresnel reflection coefficient, $\varepsilon_s=\varepsilon_s(\rho_d, m_v, T_s, C)$ is the soil complex permittivity, ρ_d is the soil bulk dry density, m_v is the volumetric soil moisture, C is the soil texture factor (clay or organic content), and h_r is a parameter of soil surface roughness. In this approach, we neglected wave scattering in vegetation and snow cover, and we did not consider the profiles of the permittivity and temperature in the active layer of frozen soil. Based on satellite measurements of brightness temperature and ground-based measurements of surface soil temperature (0-1cm), using the model (1), the reflectivity of the area over the FBS test site was estimated. In this way, the estimated values of soil reflectivity on horizontal and vertical polarizations depending on the surface soil temperature are depicted in Fig.1. Following the model (1), the reflectivity depends on the soil temperature only through its dielectric permittivity. In the process of freezing (surface soil temperature less than ones at the depth 8cm), as the temperature of frozen soil decreases, the volumetric content of transition water decreases, but the ice component increases. These processes lead to a decrease in the soil permittivity and, consequently, in the reflectivity of the soil, as can be seen in Fig. 1 as the surface soil temperature decreases.

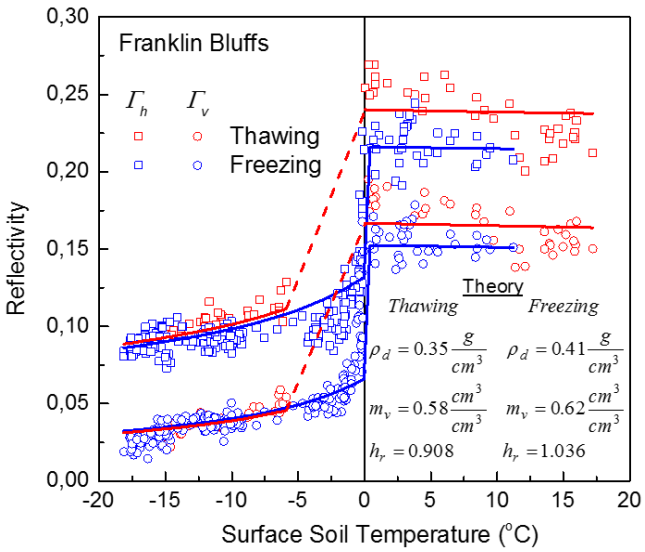

Fig. 1. Soil reflectivity at the FBS test site depending on surface soil temperature, measured by the FBS weather station in 0-1cm layer. The values of brightness temperature measured by the SMAP radiometer and calculated ones are depicted by symbols and lines respectively. "Thawing" and "Freezing" in figure signify that surface soil temperature (0-1cm) was more and less, respectively, than soil temperature at the depth of 8cm according to the weather station data.

In the next step of the analysis, we will try to theoretically describe the experimentally established temperature dependence of the reflectivity due to only the temperature variations of the surface soil permittivity. To this end, the inverse problem relative to moisture content, density and roughness of the soil surface at the FBS test site using emission model (1) was solved. The inverse problem was solved by minimizing the residual norm between the time series of brightness temperatures measured by the SMAP radiometer and calculated values based on formula (1) using a dielectric model [6] of organic soil. The time series data was taken for the whole year, both during the thawed and frozen soil states. The values of the optimally found

parameters during the minimization process are given in the legend to Fig. 1. The obtained values of the soil bulk dry density correspond well to the bulk dry density of the organic topsoil observed in natural conditions in the arctic tundra region. Relative to an average soil moisture of ~0.4cm^3/cm^3, measured by the FBS weather station at a depth of 18-22 cm in the period 2015-2016, the retrieved soil moisture value is partly overestimated, which indicates that water objects were not considered within the effective pixel of the SMAP radiometer (9km x 9km) in the model used (1). In accordance with the calibration dependence in article [11, see Fig. 1], the retrieved values of the soil surface roughness parameter correspond to the root-mean-square deviations of the soil surface heights which are about 3.5 cm. To minimize the effects associated with wave attenuation in the snow and vegetation cover, and also due to scattering on the soil surface roughness, the ratio between vertically and horizontally polarized reflectivities were calculated (see Fig.3) based on the data, depicted in Fig.1.

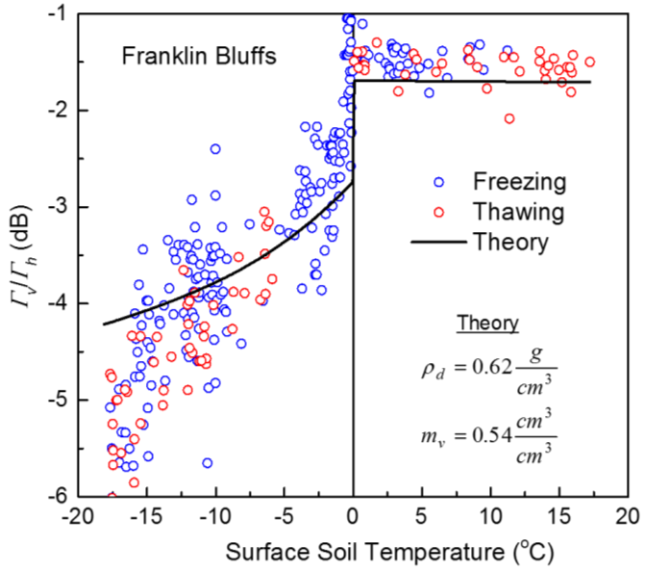

Fig. 2. Dependence between the ratio of reflectivities and soil surface temperature. The denotation "Freezing" and "Thawing" have a similar meaning as in Fig.1.

The values of soil dry bulk density and volumetric moisture were retrieved using a similar procedure to the one described above. As can be seen from Fig. 2, the most significant deviations of the measured value of reflectivity from the calculated ones are observed in the temperature range from -20°C to -10°C. From our point of view, the gradients of permittivity and temperature observed at this time in the active topsoil contribute significantly to the emission and were not taken into account in the model (1). In the temperature range from -12°C to 0°C, where the slope of the temperature dependence of the soil permittivity is significant, the temperature dependence of reflectivity can be described mainly due to the dielectric properties of the soil cover. The correlation coefficient between the measured and retrieved values of the reflectivity polarization ratio in the negative temperature region was found to be equal to 0.68. In the area of the ISA weather station, the temperature dependence of the radar backscattering coefficient measured by Sentinel-1 relative to the soil surface temperature measured by the weather station is depicted in Fig. 3. The dependence is qualitatively similar to the temperature dependence of the reflectivity ratio (see Fig. 2) which was established above on the basis of SMAP radiometric data.

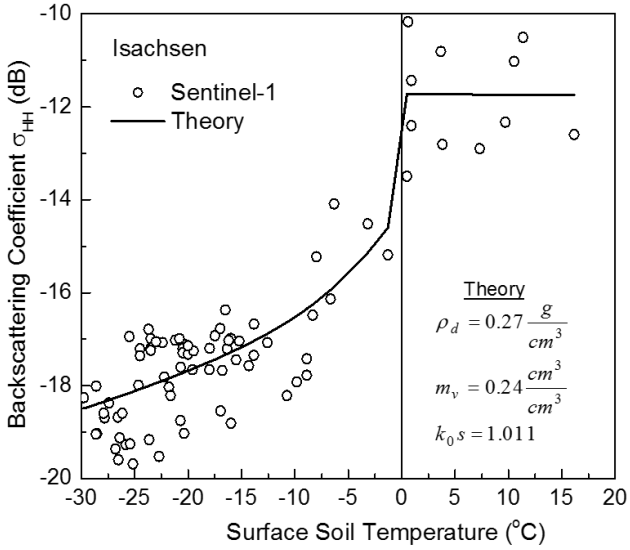

Fig. 3. Dependence between the Sentinel-1 backscattering coefficient and the soil surface temperature (0-1cm) in the area of ISA weather station.

To analyse the radar backscattering variations, *Oh's* model was used under the assumption of a dielectrically homogeneous active topsoil, without taking into account wave scattering and attenuation in the snow pack and canopy [12]:

$$\begin{aligned} \sigma_{HH} &= g\sqrt{p}\cos^3\vartheta\left[R_V(\vartheta,\varepsilon_s)+R_H(\vartheta,\varepsilon_s)\right], \\ g &= 0.7\left(1-e^{-0.65k_0 s^{1.8}}\right), \\ \sqrt{p} &= 1-(2\vartheta/\pi)^{0.314/R_0(\varepsilon_s)}e^{-k_0 s}, \end{aligned} \quad (2)$$

where ϑ is the incidence angle in radians, R_0=$R_{H,V}$(ϑ=0), k_0 is a free space wave number, and s is the root-mean-square deviation of the soil surface height. In a similar way to the analysis of radiometric data, the inverse problem concerning the soil moisture, m_v, dry bulk density, ρ_d, and roughness parameter, k_0s, while minimizing the residual norm between the time series of the backscattering coefficient measured by Sentinel-1 and the calculated ones was solved for all available data, including both thawed and frozen soil. The backscattering coefficients were calculated on the basis of the ISA weather station soil surface temperature (0-1cm) data, model (2), and the dielectric model [6], neglecting the frequency dispersion of the complex dielectric permittivity in the frequency range from 1.4 to 5.4 GHz, and snow cover (~0.2m in depth, which is mainly dry in winter and it is transparent environment for C-band). Thus, the calculated

reflection coefficient for the optimally found parameters as a function of the soil surface temperature is depicted in Fig. 3. The retrieved value of the soil dry bulk density (0.27 g/cm^3) corresponds to the ones observed in the organic topsoil in actual tundra conditions, but it in two times smaller than (0.62-0.9g/cm^3) reported in [9]. Relative to an average soil moisture of ~0.3cm^3/cm^3 measured by the ISA weather station at a depth of 11 cm in the period 2015-2016, the retrieved soil moisture value (0.24cm^3/cm^3) correlates very well. The retrieved value of root-mean-square deviations of the soil surface heights (s=0.01cm) corresponds to a flat landscape in the vicinity of the ISA weather station installation. The correlation coefficient between the measured and retrieved values of the backscattering coefficient in the negative temperature region was found to be equal to 0.73. It can also be concluded that the temperature dependence of the backscattering coefficient for arctic tundra soil almost without vegetation can be described with a good degree of accuracy only due to temperature changes in the dielectric permittivity of the topsoil.

5. CONCLUSION

In this paper, the temperature dependences of the reflectivity, measured by a SMAP radiometer, and backscattering coefficient, measured by Sentinel-1, in the process of the heating and cooling of frozen soil for two typical tundra test sites located in the North Slope of Alaska near Franklin Bluffs meteorological station and on Ellef Ringnes Island near Isachsen weather station were investigated. As a result, it was shown that in the range of soil surface temperature changes from -30°C to 0°C, the variations of the backscattering coefficient and reflectivity are about 4 dB for both test sites. It is shown that these changes are mainly due to the temperature dependence of the soil permittivity with a high content of organic matter. The experimentally confirmed temperature dependence of the reflectivity and backscattering coefficient from satellite observations opens up the possibility of measuring such important parameters as the unfrozen water content in frozen Arctic soil, and more accurate approaches to identifying frozen and thawed soil states can be developed. In addition, the possibility of estimating the annual average parameters such as soil density, surface soil moisture and roughness has been demonstrated. Further research is planned for other test sites in order to investigate the possibility of establishing temperature dependencies for different landscape conditions in the Arctic tundra region.

6. ACKNOWLEDGEMENT

The study was performed thanks to a grant from the Program of SB RAS II.12 (№0356-2017-0034) and project № 0356-2018-0060.

7. REFERENCES

[1] World Meteorological organization [Online]. Status of the Global Observing System for Climate (GCOS-195), October 2015. Available: http://www.wmo.int/pages/prog/gcos/Publications/GCOS-195_en.pdf.

[2] Rautiainen K., et al. "SMOS prototype algorithm for detecting autumn soil freezing," Remote Sensing of Environment, vol. 180, pp. 346-360, 2016.

[3] Al-Yaari A. et al. "Global-scale evaluation of two satellite-based passive microwave soil moisture datasets (SMOS and AMSR-E) with respect to Land Data Assimilation System estimates," Remote Sensing of Environment, vol. 149, pp. 181-195, 2014.

[4] Roy A. et al. "Response of L-Band brightness temperatures to freeze/thaw and snow dynamics in a prairie environment from ground-based radiometer measurements," Remote Sensing of Environment, vol. 191, pp. 67-80, 2017.

[5] Muzalevskiy K. V. and Z. Ruzicka, "Retrieving Soil Temperature at a Test Site on the Yamal Peninsula Based on the SMOS Brightness Temperature Observations," in IEEE Journal of Selected Topics in Applied Earth Observations and Remote Sensing, vol. 9, no. 6, pp. 2468-2477, 2016.

[6] Mironov V.L., Savin I.V. "A temperature-dependent multi-relaxation spectroscopic dielectric model for thawed and frozen organic soil at 0.05–15 GHz," Physics and Chemistry of the Earth, Parts A/B/C, vol. 83-84, pp. 57-64, 2015.

[7] Rodionova N.V., "Sentinel-1 data correlation with ground measurements of soil temperature," Sovremennye problemy distantsionnogo zondirovaniya Zemli iz kosmosa, vol. 14, No. 5, pp. 135-148, 2017.

[8] Khaldoune J., et al., "An approach for mapping frozen soil of agricultural land under snow cover using RADARSAT-1 and RADARSAT-2, " IEEE Geoscience and Remote Sensing Symposium Proc., 2008, Vol. 3, pp. III-382–III-385.

[9] Vonlanthen, C.M., Raynolds, M.K., Munger, C.A., Kade, A.N., Walker, D.A. 2006. Biocomplexity of Patterned Ground Isachsen Expedition, July 2005. AGC Data Report. University of Alaska Fairbanks, Fairbanks, AK, 86 pp.

[10] Permarfrost Laboratory University of Alaska. [Online]. Database. Available: http://permafrost.gi.alaska.edu/site/fbw (/isa).

[11] Wigneron J.-P., et al., "Modelling the passive microwave signature from land surfaces: A review of recent results and application to the L-band SMOS & SMAP soil moisture retrieval algorithms," Remote Sensing of Environment, vol.192, pp. 238-262, 2017.

[12] Y. Oh, K. Sarabandi and F. T. Ulaby, "An empirical model and an inversion technique for radar scattering from bare soil surfaces," in IEEE Transactions on Geoscience and Remote Sensing, vol. 30, no. 2, pp. 370-381, Mar 1992.